

# The effect of degradation on the structural response of a reinforced concrete arch bridge

Paolo Andrea Miglietta<sup>1</sup>, Gianni Blasi<sup>1</sup>, Daniele Perrone<sup>1</sup>, Francesco Micelli<sup>1</sup>,  
Maria Antonietta Aiello<sup>1</sup>

<sup>1</sup>*Department of Engineering for Innovation,  
University of Salento,  
Via per Monteroni, Lecce (73100), Italy*

## Abstract

In recent years, several bridge collapses have occurred worldwide, resulting in human life and economic direct and non-direct losses. Such events are likely related to the age of bridges, which is approaching their lifespan in most of the cases. Furthermore, older bridges were designed according to outdated standards and built by using outdated materials and technologies, and consequently, require major retrofitting. Since infrastructures play a fundamental role in the road network, stakeholders and governance are committed to improve their performance with urgency. Structural safety assessment is fundamental to properly plan and identify maintenance interventions, also accounting for the effects of degradation phenomena. In fact, steel reinforcement corrosion, concrete cracking, creep and shrinkage severely affect expected lifespan of a structural system exposed to external environment and fatigue loads. In this paper, a review of the degradation models available in the literature is provided, discussing the influence of the main parameters on each degradation phenomenon. Subsequently, a numerical model of a case study Maillart's bridge located in southern Italy is developed, implementing degradation effects to assess their influence on the structural performance. Since the bridge is located nearby the coast, both carbonation and chloride-induced corrosion of reinforcement were considered, as well as long-term physical effects on concrete mechanical behaviour. The results showed that material degradation may influence both local and global response of the structure and that predicting bridge behaviour evolution over time can be useful for its life cycle management.

## 1 Introduction

Recent bridge collapses have focused the attention of stakeholders on the health of infrastructures and on their need for maintenance. In Italy, many infrastructural assets (e.g. bridges, tunnels) were built over than fifty years ago, according to outdated standards and materials. Consequently, they are approaching their lifespan end or require retrofitting [1]. Despite their age or health, existing infrastructures still play a strategic role in the road network and their functionality loss could have a major impact on the economy, sustainability and logistics, especially in the event of seismic emergencies.

Several studies carried out in the last decades [2]-[5] have shown that building materials are affected by degradation processes, resulting in a reduction of the load-bearing capacity and ductility of the entire structure. Since the seismic behaviour is strongly dependent on the latter, life prediction, performance monitoring and bridge maintenance have become essential to avoid brittle failures and sudden collapses.

Steel rebars and tendons corrosion represents one of the main causes of deterioration of RC structures [6]. Corrosion may occur in general or localized form; the former is related to carbonation and results in a uniform reduction of reinforcement cross-section along its length, while localized corrosion is caused by chloride penetration and induces pits and notches. In addition, localized corrosion may be accelerated by freeze-thaw cycles and de-icing if joints are not maintained or inadequate. A large number of literature studies was addressed at modelling the phenomenon of corrosion and its consequences in RC structures. Particularly, degradation models [7], functionality curves [8], [9] and time-dependent N-M interaction curves for piers [10] were developed. The outcome of such studies provided useful tools for maintenance planning and showed a high correlation between structural safety index and corrosion rate.

In this work, the influence of degradation phenomena on the global structural response and the load-bearing capacity of a Maillart arch bridge was evaluated. Non-linear pushdown analyses were per-

formed on the structural system, accounting for the effect of the evolution over time of several degradation phenomena. Particularly, reinforcement corrosion and concrete degradation due to cracking within the cover depth due to carbonation were considered, alongside concrete creep. The performance of the structure was computed at different time intervals starting from the construction year, in order to compute functionality curves.

## 2 Degradation models considered

The structural response of reinforced concrete (RC) structures is deeply influenced by degradation phenomena affecting the mechanical properties of both steel and concrete. The hydration products of cement induce a high alkaline environment in concrete. Therefore, for PH higher than a specific threshold (generally around 11.5), steel reinforcements are surrounded by an iron oxide film that provide protection from corrosion. When carbon dioxide and moisture penetrate within concrete pores, the carbonation reaction occurs, neutralizing the alkalinity of the concrete. Although the mechanical properties of concrete are not directly affected by carbonation products, as carbonation reaches the concrete-reinforcement interface, the protective film is destroyed, leading to corrosion. Consequently, reduction in rebars-cross sectional area and mechanical properties decay occurs. Additionally, the production of expansive products induces tensile stress on concrete surrounding the reinforcement, leading to progressive increase of cracking up to cover spalling [6].

Carbonation penetration can be evaluated with equation (1):

$$s = K\sqrt{t} \quad (1)$$

where  $s$  is the carbonation depth in millimetres,  $t$  the time in years and  $K$  the carbonation rate in  $\text{mm/year}^{0.5}$ , which ranges between 2 for well compacted concrete and 15 for poor quality concrete. In this study  $K=7$  was assumed. Substituting the concrete cover thickness in equation (1), the corrosion initiation time can be estimated.

Once carbonation-induced corrosion was triggered, the reduction in cross-section diameter may be assessed through the corrosion rate  $v_{\text{corr}}$ . Since the chemical corrosion reaction requires water and oxygen, the corrosion rate is highly dependent on the water content within concrete pores. In fact, the corrosion rate is lower than  $1 \mu\text{m/year}$  and, consequently, can be neglected if concrete pores are dry or saturated. On the other hand, if the relative humidity (RH) is between 90% and 100%, corrosion rate may increase up to  $100 \mu\text{m/year}$ . Since the RH of the case study bridge environment is approximately 80%,  $v_{\text{corr}} = 15 \mu\text{m/year}$  was assumed [6].

As said before, both the properties of reinforcing steel and concrete are affected by corrosion of the reinforcement. A significant reduction of tensile strength, yielding strength and ductility is observed for rebars, while cracking due to expansive products of corrosion cause concrete compressive strength decay. The relationships proposed by Imperatore et al. [11] was employed herein to account for rebars properties decay, as shown in eq. (2)-(4).

$$f_{y,\text{corr}} = (1 - 0.0143453 \cdot M_{\text{loss}} [\%]) \cdot f_y \quad (2)$$

$$f_{t,\text{corr}} = (1 - 0.0125301 \cdot M_{\text{loss}} [\%]) \cdot f_t \quad (3)$$

$$\varepsilon_{u,\text{corr}} = e^{-0.0546993 \cdot M_{\text{loss}} [\%]} \cdot \varepsilon_u \quad (4)$$

where  $f_y$ ,  $f_t$  and  $\varepsilon_u$  are the uncorroded yield strength, the uncorroded tensile strength and the uncorroded ultimate strain respectively; while  $f_{y,\text{corr}}$  is the corroded yield strength,  $f_{t,\text{corr}}$  is the corroded tensile strength and  $\varepsilon_{u,\text{corr}}$  is the corroded ultimate strain; which are evaluated as a function of the percentage of mass loss  $M_{\text{loss}}$ . It is noteworthy that tensile strain, which decays according to an exponential law, is the most affected parameter in case of corrosion and can induce a wide reduction in local and global ductility.

The concrete compressive strength decrease is computed with the equation (5), proposed by Vecchio and Collins and modified by Coronelli and Gambarova [12]:

$$f_c^* = \frac{f_c}{1 + K \frac{2\pi X n_{\text{bars}}}{b \varepsilon_{c2}}} \quad (5)$$

Where  $f_c^*$  is the corroded compressive strength,  $f_c$  the uncorroded compressive strength,  $K$  a constant equal to 0.1 for medium rebar,  $X$  the corrosion penetration in mm,  $b$  the width of the cross-section in mm,  $n_{bars}$  the number of steel reinforcement in the compressive zone and  $\varepsilon_{c2}$  the strain at the peak.

Lastly, creep effect should be considered when analysing long-term evolution of structural performance, particularly in case of bridges subjected to high static and dynamic loads, which lead to progressive increase of strain. Creep is evaluated through the relationship proposed by Model Code [13], as shown in eq (6):

$$E_c(t) = \frac{E_{ci}}{\varphi(t, t_0)} \quad (6)$$

where  $E_{ci}$  is the modulus of elasticity at 28 days and  $\varphi(t, t_0)$  is the creep coefficient, depending on the geometry of the cross-section of the considered element, the RH and the mean compressive strength of the concrete ( $f_{cm}$ ). Further details on  $\varphi$  evaluation may be found in [13].

### 3 Description of the case study bridge

The bridge analysed in this study is located in the south-east coast of Salento (Apulia, Italy) and was built in 1967. The original structure consists of a thin RC arch connected to the upper deck through vertical trusses, as depicted in Fig. 1 (left). The arch span and depth are equal to 44 m and 7 m, respectively, while its thickness varies from 250 to 300 mm. Such thickness value was designed in order to avoid buckling phenomena and reduce as much as possible the self-weight of the vault. The upper deck is 7 m wide and consists of a thin slab supported by four longitudinal beams with cross-section equal to 250x1000 mm. Each vertical truss connecting the arch to the deck is characterized by either a set of four columns (at the ends) or a thin wall (in the mid-span). Spandrel beams are used at the ends of the trusses for the connection to the arch and the deck [14].

The high flexural stiffness of the deck leads to negligible bending moment in the vertical elements. As a result, the arch behaves as a fully compressed element under dead loads. The foundation elements of the arch are plinths. The deck is constrained at the abutments on one side by a hinge and on the other by a roller, to allow for longitudinal displacements caused by thermal loads. Two access girders, 6.15 m and 9.75 m long respectively, connect the bridge to the abutments and are constrained to the main structure with half-joints.

The characteristic compressive strength of concrete,  $f_c$ , is equal to 25 MPa for foundation elements and 30 MPa for both the arch, columns and girders 30 MPa. Smooth steel rebars were used for concrete reinforcement, having yielding strength  $f_y=310$  MPa, tensile strength  $f_t=600$  MPa and ultimate strain  $\varepsilon_u=10\%$  (Aq60 grade). All structural elements have a concrete cover equal to 25 mm.

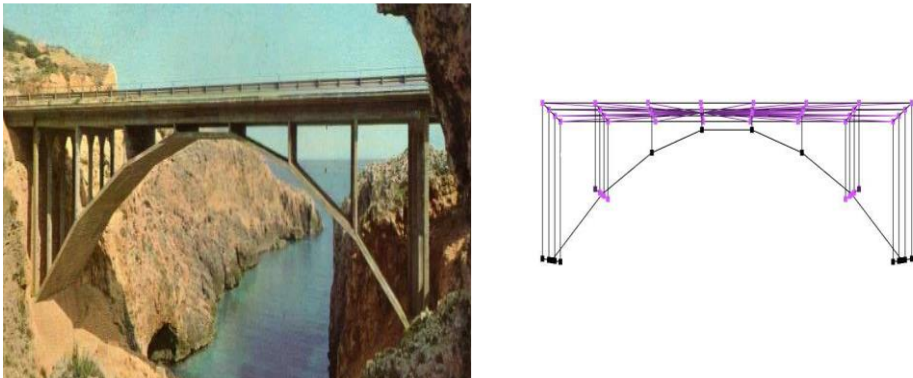


Fig. 1 The “Ciolo” Bridge in 1967 (left) and the numerical model of the “Ciolo” bridge (right).

#### 3.1 Description of the numerical model

The finite element model of the case study bridge was realized in STKO [15]. The structural elements were modelled using beam elements, except for the upper slab, which was simulated including rigid

diaphragm constraints for the deck beam, as shown in Fig. 1 (right). For the sake of simplicity, the geometric details of structural elements, such as rings and countersinks, were neglected in this study. Pinned restraints ( $U_x$ ,  $U_y$  and  $U_z$ ) were included at both ends of the arch and of the slab to simulate boundary conditions furthermore, access ramps were neglected in this study. Additionally, spandrel beams were assumed as rigid elements, by setting equalDOF constraints at all their nodes.

The mechanical behaviour of the arch, the struts and the deck beams was simulated through a smeared plasticity approach, adopting fiber-based non-linear beam elements. The stress-strain relationship of materials characterizing fiber sections was defined using Concrete02 and hysteretic mechanical model for concrete and steel rebars, respectively. Referring to spandrel beams, elastic beam elements were used.

### 3.2 Modelling of degradation phenomena

According to Tuuti's model [16], the service life of the structure exposed to corrosion can be divided into two periods: the trigger period and the propagation period, as shown in Fig. 2 (left). During the trigger stage, corrosion penetration is zero and only concrete creep occurs. In the propagation stage corrosion takes place, resulting in loss of the reinforcement cross sectional area and in the decay of the mechanical properties of steel, as shown in Fig. 3 (left and right). For the considered elements, the corrosion initiation time,  $t_{corr}$ , was computed by substituting the depth of concrete cover in (1). Since all elements had the same concrete cover depth, the resulting value of  $t_{corr}$  was equal to 12 years.

In order to account for concrete creep, a time-dependant reduction factor for Young's modulus was used, as shown in equation (6). The evolution of the elastic modulus is depicted in Fig. 2 (right).

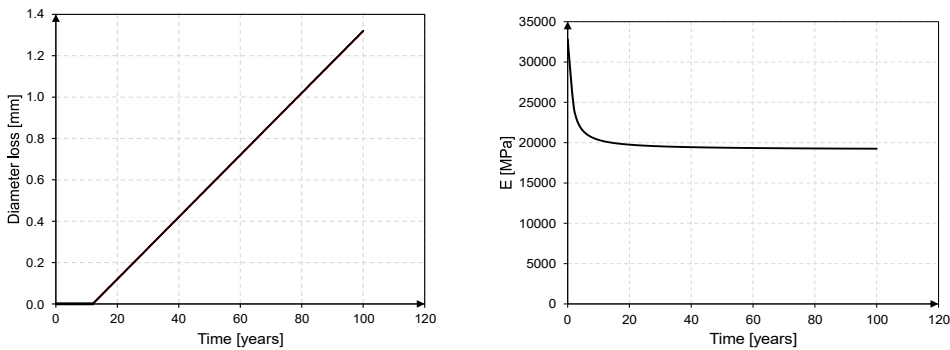


Fig. 2 Trigger period and propagation period for the “Ciolo” bridge (left). Decay of elastic modulus due to creep (right).

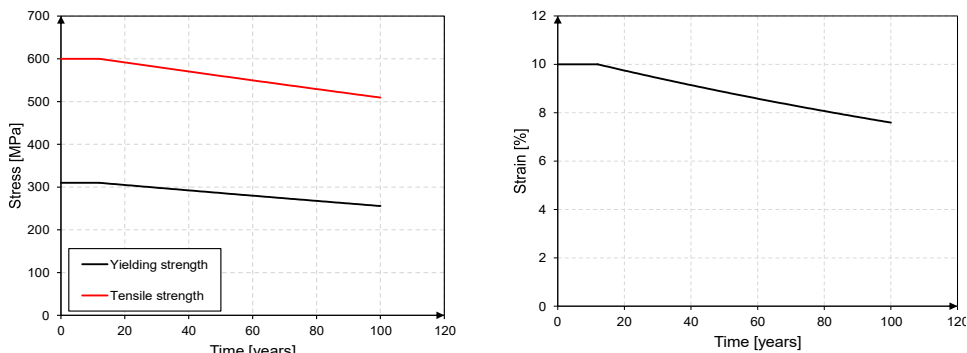


Fig. 3 Decay of yielding strength and tensile strength of the steel (left). Decay of ultimate strain of the steel (right).

As said before, concrete region surrounding reinforcement bars is affected by corrosion. To account for this aspect, the cross-sections of elements were divided into two regions: an inner core and a degraded region, including the concrete cover and an inner layer with depth equal to twice as the rebar diameter, as suggested by [10]. An example of such partition is depicted in Fig. 4 (left), where the green layer represents the degraded region and the grey area is the un-degraded inner core. Recent studies showed that the degraded area of the concrete should be defined through a circle having centre corresponding to the reinforcement rebar axis and with diameter equal to the depth of the cover [17], however, a more conservative and simplified approach was adopted in this study. The adopted approach allowed modifying the mechanical behaviour of the outer region of concrete cross-section depending on the corrosion penetration, as shown in Fig. 4 (right). On the contrary, the mechanical behaviour of the inner core was kept constant.

In summary, only the elastic modulus of concrete was reduced over time until the time of corrosion initiation, whereas both mechanical properties of steel and concrete in the outer region were reduced during the propagation period.

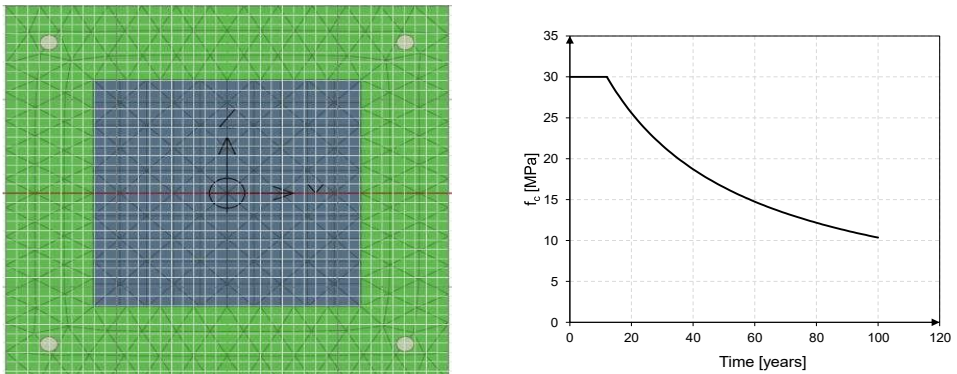


Fig. 4 Cracked region (green) and inner core (grey) for the cross-section of a square column (left) and decay of concrete compressive strength (right).

## 4 Numerical analysis of the bridge

With the aim to evaluate the structural behaviour as a function of degradation phenomena, non-linear Push-down analyses were carried out on the bridge at different time periods starting from construction time.

Firstly, a gravity load analysis was performed considering both the structural and non-structural dead loads and a live load equal to  $8 \text{ kN/m}^2$ , as defined by the Italian building design code [18]. Since the upper slab was not explicitly modelled, its relative non-structural and live loads were applied to the longitudinal beams, according to the tributary length method. As a result, the sum of dead and live loads was equal of  $17.6 \text{ kN/m}$  and  $8.8 \text{ kN/m}$  for central and side beams, respectively. At the end of the gravity load analysis, the push-down analysis was carried out using a loading protocol with magnitude proportional to that of the sum of dead and live load. The push-down load value was increased up to structural collapse. Further details of the analysis performed are provided in the following.

### 4.1 Push-down analysis setting

The push-down analysis was performed in displacement control, by setting the control node at the top of the arch. The adoption of displacement-controlled protocol allowed to detect the post peak branch in the load-displacement curve, in order to reliably assess the achievement of collapse. An example of the obtained pushdown curve is depicted in Fig. 5 (left). Because of the static scheme of the bridge analysed, the response is nearly elastic up to structural failure. In the initial stage, only minor cracking was obtained, while structural collapse occurs because of the failure of the longitudinal beams in correspondence to the connection to central walls. Such failure mode causes a noticeable load drop in the curve.

Since the main purpose of this study is to assess the influence of the degradation phenomena on the load-bearing capacity, the post-peak branch was not included in the curves discussed in the following.

As previously stated, several pushdown analyses were carried out to account for the evolution over time of degradation phenomena. Since the major decay of the elastic modulus occurs in the first years, analyses were carried out every year until the fifth year in order to detect its influence on the structural response. After this threshold, time-steps were set every five years. From year 15 to year 24, analyses were carried out every 3 years to detect the effect of the corrosion phenomenon on the load-bearing capacity. The push-down analyses were carried out up to the 24th year, since strengthening interventions were carried out on the bridge in 1992 and then the structural behaviour was modified.

The outcomes summarized in Fig. 5 (right), show that up to corrosion initiation time (grey curves) the load-bearing capacity of the bridge is almost constant however, the stiffness sharply decreases due to creep. When corrosion takes place (red curves), both load-bearing capacity and ultimate displacement decrease, due to loss of performance of the mechanical properties of materials.

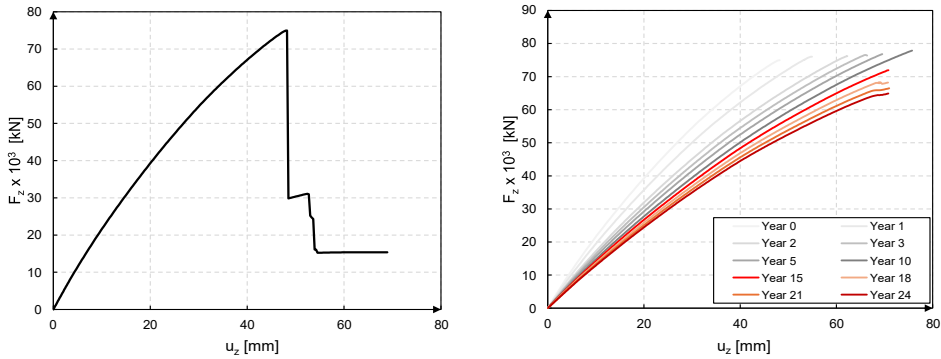


Fig. 5 Pushdown curve of the “Ciolo” Bridge in the undamaged state (left) and as a function of degradation phenomena (right).

The results obtained from the pushdown analyses were used to define the functionality curve of the case study bridge, which shows the evolution of the load-bearing capacity over time (Fig. 6). This curve may be useful to predict the performance of the bridge over time and to identify the time for required retrofit intervention, based on lower bounds of the performance level. It is worth mentioning that functionality curve was computed up to 24 years after construction (i.e. 1992), because major strengthening interventions were carried out between 1992 and 1994. The presence of such interventions leads to a “jump” in the curve in correspondence to the retrofit year and was neglected in this study. Future works will be addressed at computing functionality curve evolution after retrofit time.

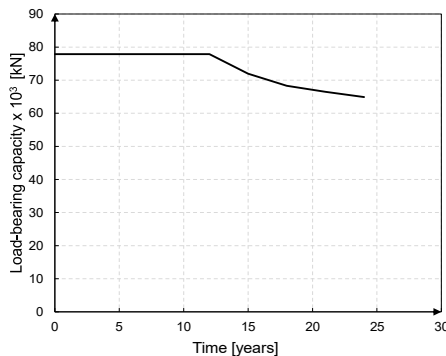


Fig. 6 Functionality curve of the “Ciolo” Bridge.

## 5 Conclusions

In this study, a simplified model with embedded damage of a RC arch bridge located nearby the coast was developed, aiming to define the structure functionality curve. The outcomes confirmed that the reinforcement corrosion is the main cause of degradation in RC structures, and it is closely related to construction details and quality of materials, such as cover depth and concrete porosity. Particularly, no losses in load-bearing capacity were detected in the functionality curve up to the triggering time. In fact, the only mechanical property decay within the triggering period is related to creep, which only affects global stiffness. After corrosion initiation time, load bearing capacity is related to cross-sectional area reduction of reinforcing rebars.

The functionality curve developed may be a useful tool for stakeholders to monitor the structural performance, prioritize retrofitting and define the maintenance strategies. Several aspects of this complex and innovative topic, such as the influence of degradation processes on the seismic response and influence of strengthening interventions on functionality curves, are demanded to future works.

## Acknowledgements

This work is part of the research activity developed by the authors within the framework of the “PNRR”: SPOKE 7 “CCAM, Connected Networks and Smart Infrastructure” - WP4.

## References

- [1] Calvi, Gian Michele, Moratti, Matteo, O’Reilly, Gerard J., Scattarreggia, Nicola, Monteiro, Ricardo, Malomo, Daniele, Calvi, Paolo M., and Rui Pinho. 2018. “Once upon a Time in Italy: The Tale of the Morandi Bridge.” *Structural Engineering International*, 29:198–217.
- [2] Andrade, Carmen. 2019. “Propagation of reinforcement corrosion: principles, testing and modelling.” *Materials and Structures* 52.
- [3] Pedrosa, Filipe and Carmen Andrade. 2017. “Corrosion induced cracking: Effect of different corrosion rates on crack width evolution.” *Construction and Building Material* 133:525-33.
- [4] Andrade, Carmen and Nuria Rebolledo. 2018. “Generic modelling of propagation of reinforced concrete damage.” Paper presented at the High Tech Concrete: Where Technology and Engineering Meet, Maastricht, The Netherlands, June 12-14.
- [5] Vecchio, Frank J, and Michael P. Collins. 1986. “The Modified Compression-Field Theory for Reinforced Concrete Elements Subjected to Shear.” *Journal Proceedings* 83:219-31.
- [6] Pedferri, Pietro and Luca Bertolini. 2000. *La durabilità del calcestruzzo armato*. McGraw-Hill Education.
- [7] Liu, Jinhong, Xiaoyong, Luo, and Chen Qi. 2023. “Degradation of Steel Rebar Tensile Properties Affected by Longitudinal Non-Uniform Corrosion.” *Materials* 2023 16.
- [8] Domaneschi, Marco, De Gaetano, Antonino, Casas, Joan R., and Gian Paolo Cimellaro. 2020. “Deteriorated seismic capacity assessment of reinforced concrete bridge piers in corrosive environment.” *Structural Concrete* 21:1823–38.
- [9] Loreto, Giovanni, Di Benedetti, Matteo, and Antonio Nanni. 2011. “Evaluation of corrosion effect in reinforced concrete by chloride exposure.” Paper presented at the SPIE Smart Structures and Materials + Nondestructive Evaluation and Health Monitoring, San Diego, United States, March 6
- [10] Di Sarno, Luigi and Francesco Pugliese. 2019. “Critical review of models for the assessment of the degradation of reinforced concrete structures exposed to corrosion.” Paper presented at the Earthquake Risk And Engineering Towards A Resilient World Conference, Greenwich, London, September 9-10.
- [11] Imperatore, Stefania, Rinaldi, Zila, and Carlo Drago. 2017. “Degradation relationships for the mechanical properties of corroded steel rebars” *Construction and Building Materials* 148:219–30.
- [12] Coronelli, Dario and Pietro Gambarova. 2004. “Structural Assessment of Corroded Reinforced Concrete Beams: Modeling Guidelines.” *Journal of Structural Engineering* 130.
- [13] CEB-FIP model code for concrete structures 2010. International Federation for Structural Concrete.

- [14] Micelli, Francesco, Perrone, Daniele, and Maria A. Aiello 2023. “Correspondence Influence of strengthening interventions on the structural performance of a Maillart-type arch bridge: the case of ‘Ciolo Bridge’ in the South of Italy.” *Eurostruct* 6:89-98
- [15] Petracca, Massimo et al. 2017. STKO user manual. ASDEA Software Technology Pescara, Italy, 2017.
- [16] Tuutti, Kyosti. 1982. “Corrosion of steel in concrete.” PhD thesis, Swedish cement and concrete research institute, Lund University, Stockholm.
- [17] Felitti, Matteo, Oliveto, Francesco, Pelle, Danilo, and Filippo Valvona. 2023. Valutazione di ponti e viadotti esistenti soggetti a rischi strutturale in condizioni statiche, sismiche e di degrado. Maggioli Editore.
- [18] D.M. 17/01/2018. “Norme tecniche per le costruzioni.” Italian Ministry of Infrastructure.